NRC Publications Archive
Archives des publications du CNRC

Colloidal CdSe 0-dimension nanocrystals and their self-assembled 2-dimension structures

Liu, Yuanyuan; Zhang, Baowei; Fan, Hongsong; Rowell, Nelson; Willis, Maureen; Zheng, Xiaotong; Che, Renchao; Han, Shuo; Yu, Kui

National Research Council Canada   Conseil national de recherches Canada

Canada

Colloidal CdSe 0-Dimension Nanocrystals and Their Self-Assembled 2-Dimension Structures

Yuanyuan Liu,[†] Baowei Zhang,[†] Hongsong Fan,[‡] Nelson Rowell,[∥] Maureen Willis,[†,¶] Xiaotong Zheng,[⊥] Renchao Che,[#] Shuo Han,*[,†] and Kui Yu*[,†,‡,§]

[†]Institute of Atomic and Molecular Physics, Sichuan University, Chengdu 610065, People's Republic of China

[‡]Engineering Research Center in Biomaterials, Sichuan University, Chengdu 610065, People's Republic of China

[§]School of Chemical Engineering, Sichuan University, Chengdu 610065, People's Republic of China

[∥]National Research Council Canada, Ottawa, Ontario K1A 0R6, Canada

[⊥]Key Laboratory of Advanced Technologies of Materials, Ministry of Education, Southwest Jiaotong University, Chengdu 610031, People's Republic of China

[#]Department of Materials Science and Laboratory of Advanced Materials, Fudan University, Shanghai 200433, People's Republic of China

[¶]School of Physics and Astronomy, Queen Mary University of London, London E1 4NS, United Kingdom

S *Supporting Information*

ABSTRACT: We report on a particular type of CdSe nanocrystals (NCs) that exhibit a single optical absorption doublet. The two peaks in the doublet are relatively sharp with a full width half-maximum as narrow as 10 nm. The peak positions vary with passivation ligands (at ~426 and ~453 nm for amine ligand passivation and at ~432 and ~460 nm for carboxylate ligand passivation). To date, it has been generally concluded that these NCs have a two-dimension (2D) morphology with 1D quantum confinement. Here, we report that zero-dimension (0D) NCs with 3D quantum confinement can exhibit a very similar static optical feature consisting of a sharp absorption doublet. We show that our as-prepared CdSe NCs (without further purification) were mainly 0D NCs, as observed when they were deposited on transmission electron microscopy (TEM) grids directly from toluene or hexane dispersions. We further demonstrate that it was possible to alter this 0D morphology by using dispersion additives and/or purification solvents to result in the appearance of 2D NCs under TEM. Although the 0D and self-assembled 2D NCs displayed similar static optical features, the two morphologies behaved quite differently in polarized emission. The 2D NCs exhibited detection angle dependent polarized emission, whereas the 0D NCs do not. Our findings indicate that a well-like morphology can be induced by the presence of hexadecylamine (HDA) in the dispersion with sonication for amine-passivated 0D NCs or by the use of ethanol during purification with dispersion storage for carboxylate-passivated 0D NCs. In this way, it is possible to manipulate the NC morphology for a targeted application through the appropriate post-treatment. This study highlights that more sophisticated theoretical studies are required to account for the experimental observations in which both 0D NCs and their self-assembled 2D NC products display similar static optical features.
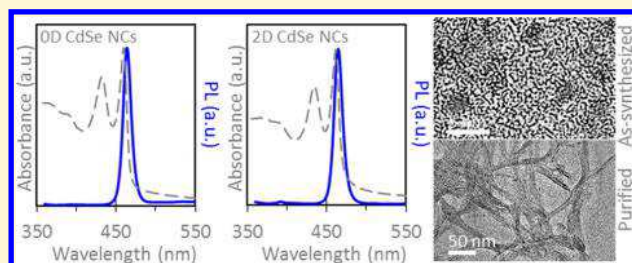
■ INTRODUCTION

Colloidal semiconductor nanocrystals (NCs) have attracted considerable attention for both fundamental and technology-oriented research. They have shown great promise to significantly impact a number of applications including those related to lasers,[1−3] light-emitting diodes (LEDs),[4−7] photovoltaics,[8−10] and bioimaging and labeling.[11−13] In recent years, advances in synthesis have led to the development of zero-dimension quantum dots (0D QDs),[14−20] one-dimension (1D) quantum wires or nanorods[21−24] and two-dimension quantum wells (2D QWs).[25−28] In particular, one special type of NCs has been synthesized that displays one sharp absorption doublet which is composed of two well-resolved electronic

transitions.[29−39] This type of NC is different from the magic-size clusters (MSCs) that usually exhibit one sharp absorption singlet, for which the full width at half-maximum (fwhm) is significantly narrower than that of conventional NCs.[39−44] As a result of their "magic" structures, which lead to low chemical potentials, MSCs possess nearly negligible size variations. Thus, there exists little spectral line broadening from inhomogeneous effects, and only homogeneous spectral line broadening

A

contributes to the optical line width observed for a MSC ensemble.[40−44]

Among the NCs that exhibit one sharp absorption doublet,[29−39] CdSe NCs have been the most studied. The fwhm in the literature for the emission of the CdSe NCs is approximately 10 nm.[29−31] This small value approaches the limit of the homogeneous spectral line broadening associated with a single CdSe 0D QD at room temperature.[30,43,44] The majority of the reports on these CdSe NCs contain direct visualization by transmission electron microscopy (TEM), from which it has been concluded that 2D NCs with 1D quantum confinement are responsible for the absorption feature observed.[29,31,35,36,38] The properties of the 2D QW structure, such as optical gain performance, have been the subject of much research.[45−48] There has been, however, a variety of TEM morphologies reported for these 2D structures, ranging from nanoribbons[29] and nanoplatelets[31,35,38] to quantum disks.[36] As it is still not clear how to rationalize such a wide variety of structures from the synthesis methods employed, it is of importance that we understand more accurately and fully the structure and morphology of these NCs exhibiting one sharp absorption doublet. Extending this understanding is what we endeavor to do in the present study.

Regarding the TEM visualization, several important effects have remained unexplained. For example, various solvents have been used in both the process of sample purification and TEM grid preparation. Furthermore, before TEM grid preparation, a varying degree of dispersion sonication or sample storage in dispersion was generally performed. Not only did the solvents used in these processes have an apparently uncontrolled influence on what was seen in TEM visualization, but also the dispersion sonication or storage time. Let us examine the nanoribbon structure passivated by amine ligands, which was the first 2D QW reported based on TEM visualization.[29] In this case, prior to collecting optical absorption data and preparing a TEM grid from which the morphology was determined, the as-synthesized NCs were purified. The purification was performed with excess ethanol (EtOH) containing tri-n-octylphosphine (TOP). The purified NCs were dispersed in a mixture of chloroform (CHCl$_3$) and hexadecylamine (HDA, with a melting point of ~44 °C) and sonicated. The study concluded that the origin of the absorption spectrum were 2D nanoribbons, which exhibited two distinct peaks at 423 and 449 nm.[29] However, the effect of HDA on the TEM morphology was not reported, together with the sonication performed.

Two further examples of reported 2D structures are the nanoplatelets[31,35,38] and quantum disks,[36] both of which were passivated by carboxylate ligands and displayed an absorption doublet with peaks at ~433 and ~463 nm. There has been some doubt that 2D QWs are the exclusive origin of this absorption doublet, as similar absorption spectra have been reported for unpurified NCs which were claimed to be 0D.[30,32,37] The identification of the 0D NCs was mainly based on 2D diffusion ordered spectroscopy (DOSY),[32] although both dot-like and well-like NCs were seen under TEM.[30,32,37] One common theme is that the studies detecting 2D QW structures have employed short-chain alcohols, ethanol (EtOH)[31,35,36,38] or methanol (MeOH),[30,32,37] as the precipitants in sample purification. These short-chain alcohols have been shown to be able to strip carboxylate ligands from CdSe conventional NCs.[49,50] It is, therefore, reasonable that the use of the short-chain alcohols during purification could have

resulted in a similar disruption of the surface ligands of the CdSe NCs. In turn, an increase of the surface energy could cause the as-synthesized 0D NCs to form, by self-assembly, the variety of the 2D QW structures reported. It is likely that the nature of the precipitant strongly influences the resultant morphologies. It is this hypothesis that is evaluated experimentally in this work.

Here, we report that both 0D NCs and their self-assembled 2D NCs exhibited highly similar optical absorption doublets, together with the effects of HDA and of purification with EtOH on the TEM morphologies of the CdSe NCs passivated by amine and carboxylate ligands, respectively. We show that without purification, our as-synthesized NCs in toluene or hexane exhibit a sharp absorption doublet, and that they are 0D nanostructures when imaged under TEM. For the 2D structures observed under TEM, we demonstrate that they can be resulted from post treatment including dispersion sonication and storage prior to deposition onto TEM grids. Polarized emission experiments demonstrated that the as-synthesized 0D and purified 2D NCs (with EtOH instead of CH$_3$CN[49−51]) (passivated by carboxylate ligands) have different structural anisotropy, consistent with our TEM results. When the size of 0D NCs was calculated from the lowest-energy absorption peak position of the absorption doublet using two empirical equations,[52,53] we obtained about a 2 nm size, which is in agreement with our TEM study. Thus, the conclusion is supported that a 0D structure can also be responsible for the observed absorption doublet. The 0D structure can self-assemble into 2D structure. The work presented here sheds light on how dispersion and purification influence the apparent TEM morphologies, which vary from 0D NCs to 2D NCs. The control of such a process of morphological changes provides a means to manipulate NC morphologies through post-treatment methodology (including solvents combined with sonication and storage) with the view to target applications. In addition, the present study provides evidence that we need more sophisticated theoretical models for the optical properties, in which both 0D NCs and their self-assembled 2D products display similar static optical features but different detection angle dependence of polarized emission.

■ RESULTS

Amine-Passivated CdSe NCs. The reaction of CdCl$_2$ (1.50 mmol) and octylammonium selenocarbamate (4.50 mmol) in octylamine (OTA) at 70 °C was reported to result in nanoribbon-based 2D QW structures.[29] In order to verify the role of HDA on the TEM morphology, we followed the synthetic approach.[29] Figure S1-1 shows that 0D NCs were imaged from a hexane dispersion without sonication (Figures S1-1 b1 and c1), whereas 2D structures were observed when HDA was added in dispersion (Figures S1-1 b2−e2).

Given this result, we tried to modify the synthesis to achieve a shorter reaction period with little Se precursor left. The experimental conditions of the present and previous approaches toward making amine-passivated CdSe NCs are summarized in Table S1-1 in the Supporting Information. The primary differences between the two approaches were in the feed molar ratio of Cd to Se (3 to 1 versus 1 to 3) and the reaction temperature (120 °C versus 70 °C). With the modified approach, the reaction time was shortened to 90 min (from 360 min) and the Se precursor seemed to react completely. Thus, no TOP was used during purification.

Figure 1a presents the normalized absorption and photoluminescence (PL) spectra of our as-synthesized CdSe NCs
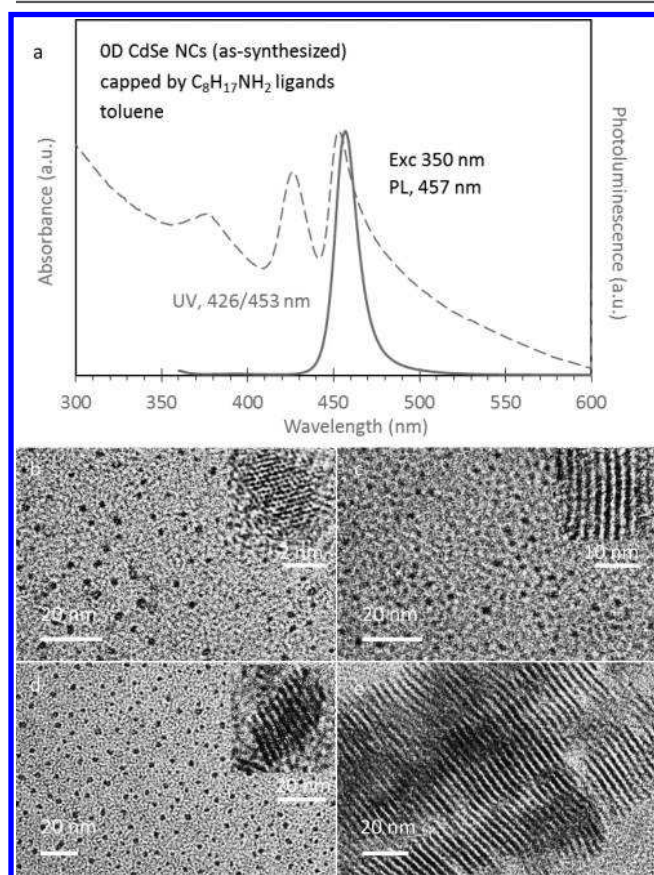
Figure 1. (a) Normalized absorption (dashed line, left y axis) and emission (solid line, excited at 350 nm, right y axis) spectra of our as-synthesized CdSe NCs from our modified reaction batch with the 3Cd−1Se feed molar ratio and Se of 1.5 mmol in 15.0 mL of OTA. The growth of the CdSe sample was at 120 °C for 90 min. The bandgap absorption and emission of the as-synthesized CdSe NCs (10 μL) without purification dispersed in 3.0 mL of toluene was at 453 and 457 nm, respectively. TEM images were from one as-synthesized sample (10 μL unpurified) dispersed in 3.0 mL of hexane before (b) and after a 30 min sonication (c), and from another 10 μL portion that was purified three times (each with 3.0 mL of EtOH) and then dispersed in 3.0 mL of CHCl$_3$ with 0.010 g of HDA before (d) and after a 30 min sonication (e). All the scale bars of the four TEM images are 20 nm, whereas those of the insets are 2 nm (b), 10 nm (c) and 20 nm (d). Image (e) seems similar to ref 29 Figures S1a and S3b. 0D structures were mainly seen from Dispersions b, c and d. 2D well-like structures were seen for Dispersions c and d, whereas dominated for Dispersion e. Clearly, the presence of HDA (d and e) together with sonication (c and e) favors the assembly of 0D NCs into 2D wells.

dispersed in toluene (Tol) (without sonication). The absorption spectrum in Figure 1a exhibits a sharp and intense absorption doublet with the first and second excitonic transitions at 453 and 426 nm, respectively. These two peak positions are 3 to 4 nm red-shifted from the values of 449 and 423 nm, which were reported for the absorption doublet of the purified CdSe NCs dispersed in a mixture of CHCl$_3$ and HDA with sonication.[29] Due to the poor dispersity in toluene of the unpurified CdSe NCs passivated by OTA ligands, a 30 min sonication was performed. The absorption spectra before and after sonication are as shown in Figure S1-2a. The sonication

promoted the dispersity, with significant increase of optical density and approximately a 2 nm blue shift in the absorption.

We further performed purification without the use of TOP. To ensure the highest level of uniformity and consistency, we fixed the amount of a sample (10 or 15 μL) with 3.0 mL of solvent across all measurements and post treatment. Upon purification, the absorption doublet was observed to slightly blue shift (as demonstrated by Figures S1-3 and S1-4 blue traces). Further dispersion sonication (Figures S1-3 and S1-4 red traces) resulted in additional blue shift of the absorption doublet to ∼449 and ∼422 nm, together with an increase of optical density. Our as-synthesized sample (10 μL) was purified three times with the mixture of 2.0 mL Tol−1.0 mL EtOH. The dispersions (3.0 mL) used for the measurements shown in Figure S1-3 were Tol (left), Tol−OTA (middle), and Tol−HDA (right), whereas those shown in Figure S1-4 were CHCl$_3$−OTA (left) and CHCl$_3$−HDA (right). The absorption doublet positions of the red spectra are almost identical to the absorption doublet at 449 and 423 nm reported in ref 29.

Figures 1b−e present the TEM images of the NCs from our modified approach. In each case, TEM grids were carefully prepared from a single 10 μL of the as-synthesized sample dispersed in 3.0 mL of solvent, either without (Figure 1b,c) or with purification (Figure 1d,e). More specifically, the grids for the images in Figure 1b,c were prepared from the same hexane dispersion before and after 30 min of sonication, respectively. The grids imaged in Figure 1d,e were prepared from the same dispersion of a mixture of 3.0 mL of CHCl$_3$ with 0.010 g of HDA before and after 30 min of sonication, respectively. The composition of the mixture of CHCl$_3$ and HDA was the same as that previously used.[29]

Figure 1b would suggest that the as-synthesized NCs were mainly 0D with an overall size of ∼2 nm. A relatively large NC with a good degree of crystallinity can be seen in the inset. After 30 min of sonication, the majority structure was still 0D NCs as can be witnessed in Figure 1c. However, some 2D wells were also observed, as shown in the inset of Figure 1c. Additional TEM images of this hexane dispersion without and with sonication are shown in Figures S1-5a and S1-5b, respectively.

Interestingly, the purified sample without sonication would appear to be dominated by 0D NCs (Figure 1d), but with some wells also detected as shown in the inset. However, after a 30 min sonication, 2D wells were apparent as the majority structure, the image (Figure 1e) of which bears a high resemblance to those reported previously.[29] The corresponding absorption spectra are presented by the blue and red traces in Figure S1-4 (right), respectively. Clearly, the 0D NCs (Figure 1b) and 2D NCs (Figure 1e) exhibit very similar optical absorption doublets (Figures 1a and S1-4 right-red trace). Additional TEM images of the purified NCs in the mixture of CHCl$_3$ and HDA can be found in Figure S1-6a (before sonication) and Figure S1-6b (after 30 min of sonication).

To test further the primary amine effect, we replaced HDA in the CHCl$_3$ dispersion with OTA (melting point around 0 °C). In this case, the 0D structure was dominant, both before (Figure S1-6c) and after 30 min of sonication (Figure S1-6d). We also explored the effect of amine in toluene and compared it with CHCl$_3$ dispersions. Figure S1-7 presents typical TEM images of our purified NCs in five dispersions without sonication and the following results were obtained.

For the toluene dispersion (Figure S1-7a), 0D NCs dominated. When OTA was present in both the toluene (Figure S1-7b) and CHCl$_3$ (Figure S1-7c) dispersions, 0D NCs

still dominated. On the other hand, with the presence of HDA in the toluene (Figure S1-7d) and CHCl$_3$ dispersions (Figure S1-7e), both 0D and 2D NCs were observed, with 0D NCs dominating for the toluene dispersion and 2D wells for the CHCl$_3$ dispersion. Table S1-2 summarizes the TEM grid preparation conditions. From these observations, it seems reasonable that the formation of the 2D QWs was promoted by the presence of HDA together with dispersion sonication, via the self-assembly of the amine-passivated 0D NCs whose optical properties are shown in Figure 1a. Thus, it can be understood that our TEM 2D morphology was shaped by the use of HDA along with sonication, which enhanced the colloidal dispersity of the CdSe NCs. The corresponding absorption spectra of the Figure 1 TEM samples are shown in Figure S1-8.

To evaluate further the effect of dispersion solvents on the structures imaged using TEM, we extended the synthesis from amine-passivated CdSe NCs to Mn-doped CdSe NCs passivated by the same amine ligands. We followed the reaction that was reported to lead to Mn-doped CdSe 2D NCs.[54] With the reported feed molar ratio for Cd to Se of 1 to 3, our reaction was performed at 100 °C (for 15 min) instead of at 70 °C. Following the presentation format of Figure 1, the resulting optical spectra and TEM images that were collected are presented in Figure 2.

Figure 2a illustrates the normalized absorption and PL spectra collected from our purified Mn-doped CdSe NCs dispersed in the CHCl$_3$−HDA mixture and with a 30 min sonication. The as-synthesized sample (10 μL) was purified three times, each time with 3.0 mL of EtOH and ~0.100 g of TOP. A sharp absorption doublet at 447 and 421 nm was detected, together with a PL peak at 604 nm. The colloidal dispersity of the NCs seemed to be less than that of the corresponding undoped NCs. Again, sonication improved the dispersity of the purified doped NCs, as illustrated by Figure S2-1 (left) which displays enhanced optical density. Figure S2-2 shows that the PL peak shifted little with the various excitation wavelengths used (in the range from 350 to 450 nm). Figure S2-3 presents the PL excitation (PLE) spectra collected at the selected emission wavelengths in the range from 590 to 650 nm. From these observations, we conclude that the emission at 604 nm (Figure 2a) was from Mn^{2+} ions as dopants within the CdSe NCs that exhibited the absorption doublet at 447 and 421 nm (Figure 2a). Thus, it appears the CdSe NCs were successfully doped with Mn^{2+} ions at the reaction temperature of 100 °C.

Similar to the undoped CdSe NCs (shown in Figure 1), 0D structures were observed to dominate from the as-synthesized Mn-doped CdSe NCs (without purification) dispersed in hexane. A typical TEM image is shown in Figure 2b, and its inset demonstrates a good degree of crystallinity of the as-synthesized 0D NCs. In addition, when the hexane dispersion was sonicated for 30 min, 0D NCs still dominated, but with apparently larger sizes. This could possibly be caused by a self-assembly process. In the case of the purified doped CdSe NCs dispersed in the mixture of 3.0 mL of CHCl$_3$ with 0.010 g of HDA, the 0D NCs remained as the majority structure, as shown in Figure 2d. However, after 30 min of sonication, the 2D wells became the majority structure as in Figure 2e. A close examination of the TEM image suggests the center-to-center distance between two nearest wells along the [11$\bar{2}$0] direction[29] is ~3.1 nm (shown in Figure S2-4). Interestingly, the wells imaged here bear strong resemblance to those morphologies
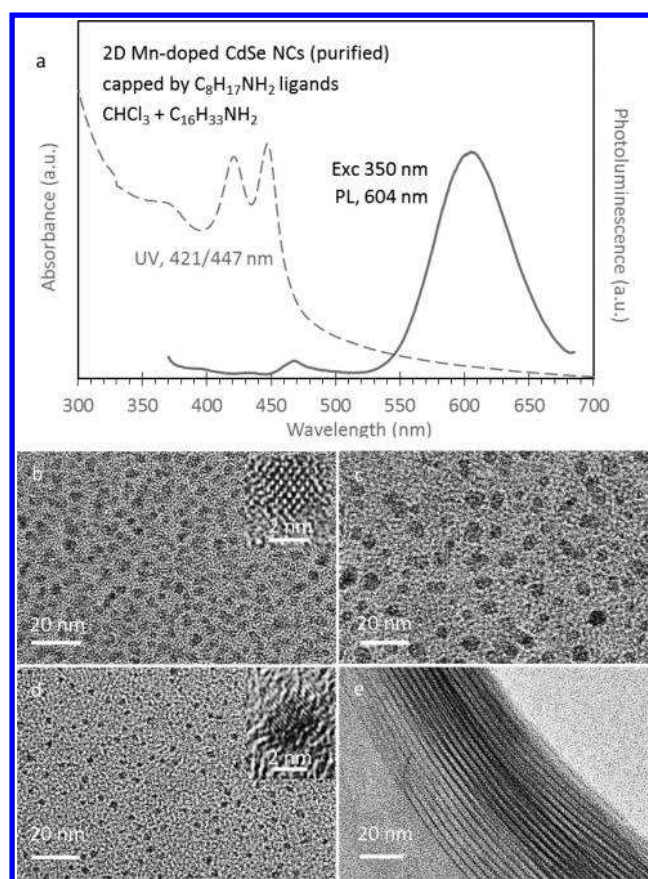
Figure 2. (a) Normalized absorption (dashed line, left y axis) and emission (solid line, excited at 350 nm, right y axis) spectra of our purified Mn^{2+}-doped CdSe NCs dispersed in a mixture of 3.0 mL of CHCl$_3$ and 0.010 g of HDA. The growth of the NCs was at 100 °C for 15 min. The TEM study was performed with unpurified NCs dispersed in 3.0 mL of hexane before (b) and after 30 min of sonication (c), and with purified NCs dispersed in the mixture of 3.0 mL of CHCl$_3$ and 0.010 g of HDA before (d) and after 30 min of sonication (e). All the scale bars in the TEM images are 20 and 2 nm for the insets. Image e looks similar to ref 54 Figure 1c. 0D NCs structures were mainly seen from the b to d images, and 2D well-like structures in the e image. Again, the presence of HDA and sonication favors the assembly of 0D NCs into 2D wells.

reported in a previous study.[54] Additional TEM images collected from these four TEM grids prepared from the two dispersions can be found in Figure S2-5. Evidently, 0D and 2D NCs were imaged from the hexane dispersion without sonication (Figure S2-5a) and from the HDA dispersion with sonication (Figure S2-5e), respectively. Again, the 0D NCs (Figure 2b) and 2D NCs (Figure 2e) exhibit a highly similar optical absorption doublet feature (Figures S2-1 (right) and 2a).

An understanding can be drawn that the well morphology of the Mn-doped CdSe 2D NCs could also have been resulted from the self-assembly of the 0D species, owing to the use of HDA and sonication, as in the undoped CdSe 2D NCs. We also tested the use of OTA and oleyamine (OLA, melting point of 21 °C) in toluene dispersion (without sonication), to compare with the result of HDA (Figure S2-6). The underlying reason for the self-assembly observed more with HDA may be related to its relatively high melting point (as compared to that of OTA or OLA). The corresponding absorption spectra of the Figure 2 TEM samples are shown in Figure S2-7. Table S2

summarizes the preparation conditions of the TEM grids for the doped CdSe NCs reported here.

Carboxylate-Ligand Passivated CdSe NCs. The first two reports describing CdSe NCs passivated with carboxylate ligands instead of amine ligands appeared in 2008, both exhibiting optical spectra with sharp absorption doublets peaked at ~463 and ~433 nm.[30,31] The absorption spectra reported are very similar, whether collected from as-synthesized CdSe samples without purification,[30] or from intensely purified CdSe samples.[31] The former report introduced a direct synthetic approach in which the coproduction of conventional QDs was eliminated.[30] This approach started with excess cadmium acetate, $Cd(OAc)_2$, in the presence of a long-chain carboxylic acid such as myristic acid (MA).[30,32,37] The essence of this direct approach was the use of low acid-to-$Cd(OAc)_2$ and high $Cd(OAc)_2$-to-Se feed molar ratios, which was successfully applied to the synthesis of other NCs including CdTe,[33] CdTeSe,[34] CdS,[40] and Cd_3P_2.[41] The latter report used an indirect approach to obtain the NCs via the separation from conventional NCs.[31,37] The indirect approach used cadmium myristate $Cd(MA)_2$ as a Cd precursor; and an acetate salt such as $Cd(OAc)_2$ or $Zn(OAc)_2$ was added at a temperature after the nucleation and growth of conventional NCs had taken place and thus the salt addition was after the induction period.[55−57] EtOH was employed to separate and purify the CdSe NC product, which exhibits one absorption doublet, from the conventional NC coproduct in a reaction batch.[31,37]

We modified the direct approach previously reported to synthesize these CdSe NCs.[30] A detailed description of this procedure for synthesis, which does not produce conventional NCs simultaneously, is provided in the Supporting Information. In essence, the modification included the use of cadmium myristate $Cd(MA)_2$ as a Cd precursor, together with the addition of acetic acid in the induction period (at 120 °C) prior to nucleation/growth of conventional quantum dots.[55−57] Figure 3a shows the absorption and PL spectra of the as-synthesized CdSe NCs (without purification) dispersed in toluene. The CdSe NCs exhibit a sharp absorption doublet peaked at 460 and 432 nm. When excited at 350 nm, the CdSe NC dispersion exhibits a narrow band gap emission peaked at 465 nm with a fwhm of ~10 nm. Here, the absorption spectrum was collected without sonication. Unlike the amine-passivated NCs, the as-synthesized CdSe NCs passivated by carboxylate ligands did not seem to improve appreciably their dispersity after a 30 min sonication (Figure S3-1). The PL excitation (PLE) study (Figure S3-1) indicated that the bandgap emission was originated from the absorption doublet.

For TEM imaging, each of the grids was prepared from a single 10 μL as-synthesized sample dispersed in 3.0 mL of solvent, with the result of the unpurified samples shown in Figure 3b−d and of the purified samples in Figure 3e−g. Before the grids were prepared, the dispersions were typically kept for only 1 min (b to e), except for those imaged in Figure 3f,g, which were kept for half a day. Figure 3b−d demonstrate that without purification, the as-synthesized NCs in hexane (b), $CHCl_3$ (c) and toluene (d) are 0D with an overall diameter of ~2 nm. The TEM image in Figure S3-2 shows that the 0D NCs are well crystallized. Additional TEM images collected from the unpurified NCs dispersions in $CHCl_3$ and in toluene are shown in Figure S3-3.

Figure 3e indicates that the purified CdSe NCs in toluene are dominated by the 0D NCs. The as-synthesized sample (10 μL) was purified three times, each time with 3.0 mL of toluene.
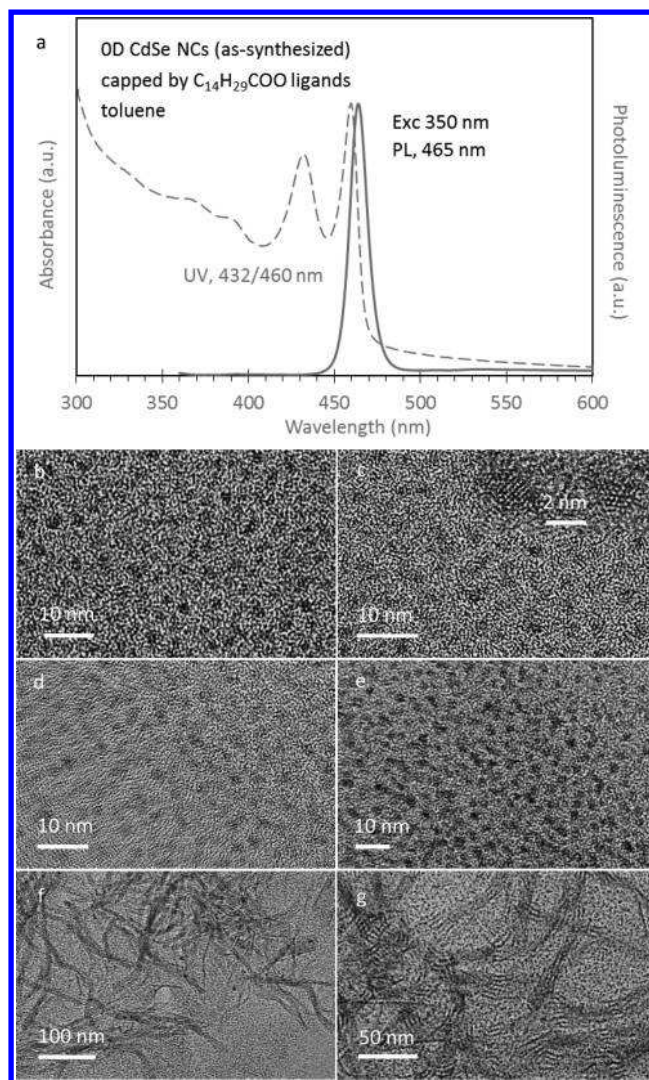

Figure 3. (a) Normalized absorption (dashed line, left y axis) and emission (solid line, excited at 350 nm, right y axis), of our as-synthesized CdSe sample (15 μL) without purification and dispersed in 3.0 mL of toluene. The sample was obtained from a reaction batch heated at 220 °C after 15 min. This reaction consisted of Cd(MA)2 (0.60 mmol) and elemental Se powder (0.15 mmol) that were mixed at room temperature in ODE, with the total weight of 4.000 g. When the temperature of the reaction mixture was heated to 120 °C, 5.00 mmol HAc in 0.700 g of ODE was added. TEM images of our as-synthesized CdSe NCs (10 μL), unpurified dispersed in 3.0 mL of hexane (b), 3.0 mL of $CHCl_3$ (c) and 3.0 mL of toluene (d), and purified (3 times, each with 3.0 mL of toluene) dispersed in 3.0 mL of toluene (e to g). The dispersions were kept for just 1 min (b to e) and for half a day (f and g) before the corresponding TEM grids were prepared. Image g looks similar to what reported in ref 62 Figure 8 and ref 38 Figure 1c.

Interestingly, we observed that the storage period of a dispersion prior to the deposition onto a TEM grid affected the morphology of the CdSe NCs imaged under TEM. When a toluene dispersion was kept for half a day prior to TEM grid preparation, 2D wells were observed to be the majority, as shown in Figure 3f,g. Additional TEM images of the purified CdSe NCs in toluene without and with increased storage time can be found in Figure S3-4. While a dispersion is being stored, it is reasonable that ligands are progressively lost from the surface of the NCs, facilitating the self-assembly of 0D NCs
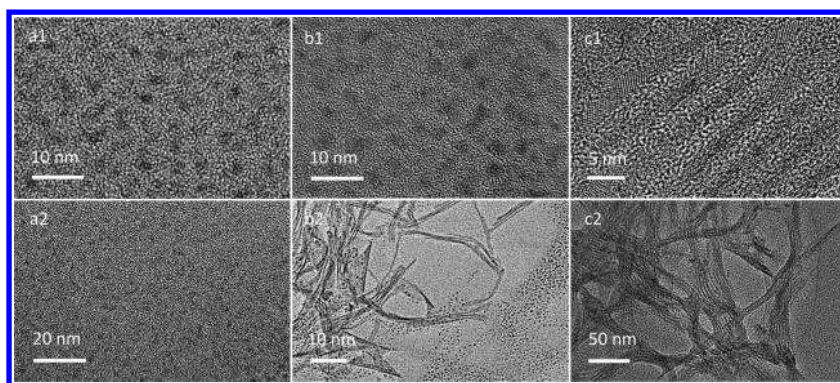
Figure 4. TEM images of the purified CdSe NCs passivated by carboxylic ligands dispersed in toluene. The purification was carried out (with 10 μL as-synthesized sample amount) three times, each with the mixture of 2.0 mL of Tol and 1.0 mL of CH_3CN (a and b), or with the mixture of 2.0 mL of Tol and 1.0 mL of EtOH (c). The TEM grids were prepared within 1 min of dispersion (a and c) and after 4 days of dispersion (b). Image c1 seems to be similar to ref 54 Figure 1d.
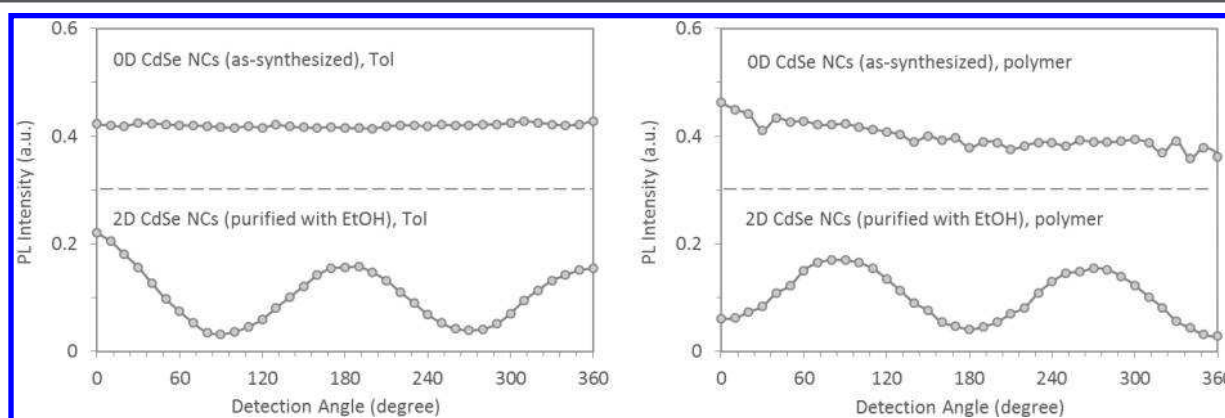

Figure 5. PL intensity as a function of detection angle (offset) for the CdSe NCs without (top traces) and with purification (bottom traces) dispersed in toluene (left) and in polymer matrix (right). The purification was carried out with a mixture of 2Tol−1EtOH. The two polymer films were stretched.[58,61] The dashed lines are just for eye guidance. A sinusoidal function fitting suggests a polarization factor P of 0.183 (left bottom trace) and of 0.142 (right bottom trace) for the purified samples. The polarization factor is defined as $P = (I_{max} - I_{min})/(I_{max} + I_{min})$.[58]

into 2D wells. It is for this reason that we prepared our TEM grids within a time as short as possible (just inside a minute), unless otherwise specified. The corresponding absorption spectra of the Figure 3 TEM samples are shown in Figure S3-5.

To study further the effect of purification on the TEM morphologies of the CdSe NCs, we used an aprotic agent (CH_3CN), to substitute the conventional protic EtOH.[31,35,36] When CH_3CN was used to precipitate CdSe NCs from their toluene dispersion, the purified NCs are 0D NCs (Figure 4a1,a2). This is probably because CH_3CN did not result in an apparent loss of the carboxylate ligands from the NC products during purification.[49−51] On the other hand, when a TEM grid was prepared 4 days later from the same toluene dispersion (Figure 4b1,b2), both 0D and 2D NCs were observed with the 0D NCs being the majority. It appears that the much longer dispersion storage time resulted in some self-assembly of the 0D NCs, similar to that shown in Figure 3f,g. Additional TEM images taken from the grid used for Figure 4b can be found in Figure S4-1a. When the protic agent (EtOH) was used, 2D wells were observed to dominate (Figure 4c), even after a short period of dispersion storage. Figure 4c1 demonstrates a good degree of crystallinity of the 2D wells. Additional TEM images obtained from the grid imaged for Figure 4c are available in Figure S4-1b.

Importantly, the absorption and emission spectra of the as-synthesized 0D NCs reported in Figure 3a are essentially the same as those obtained after purification with either CH_3CN or EtOH (Figure S4-2). The two purified samples in toluene, one with 0D structures and the other with 2D structures, showed similar band absorption doublets at ∼432 and ∼460 nm and PL peaks at 464 nm. It is thus apparent that, for the carboxylic ligand passivated CdSe NCs, the use of a protic agent such as EtOH or MeOH during purification could play a critical role in the fact that 2D wells were observed instead of 0D NCs in the TEM studies. It follows, therefore, that the 2D wells observed by TEM, the direct synthesis of which had low acid to Cd and high Cd-to-Se feed molar ratios, could have been due to the use of the protic agent during purification.[30,32] Figure S4-3 shows that the XRD patterns of the purified CdSe NCs without a protic agent were different from those with a protic agent reported.[30,36] Importantly, the supernatant and precipitant from the purification process exhibited the similar absorption doublet feature (shown in Figure S4-4), indicating that the absorption doublet should be attributed to the main, and not side, reaction product.

It has been well established that the geometric anisotropy of NCs can result in detection angle dependence of polarized PL emission,[58] similar to that of small molecules.[59,60] Figure 5 shows our polarized PL emission results for our as-synthesized and purified samples (with EtOH used in purification) with 0D
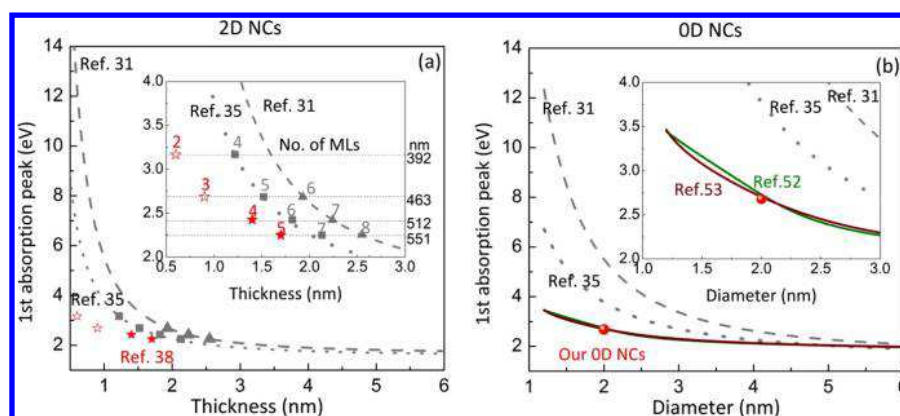
Figure 6. Two calculations with the parabolic model (the dashed gray curve, used in ref 31) and the multiband effective-mass approximation model (the dotted gray curve, used in ref 35) were performed for the 2D QW (a) and extended for the 0D NC (b), for the bandgap absorption peak (eV) vs the thickness (a) and the diameter (b), respectively. Also, the empirical equations for CdSe quantum dots reported in 2003 (the green curve, ref 52) and in 2009 (the dark red curve, ref 53) are plotted (b). For those platelets with the sharp absorption doublets at 392, 463, 512, and 551 nm, the thicknesses calculated in term of monolayers are indicated together with the solid triangles and squares, respectively. The thicknesses detected by TEM reported in ref 38 are denoted together with the solid stars and the open stars are data points derived from the result in ref 38. For the 0D NCs exhibiting the sharp absorption doublet at ∼463 nm, the size is signified with the red ball, which is in much better agreement with the two empirical equations than with the two models.[31,35,52,53]

and 2D structures passivated by carboxylate ligands, respectively. The measurements were carried out with both toluene dispersions (Figure 5, left) and polymeric films (Figure 5, right). While the polarized PL emission of the as-synthesized 0D sample (top traces) appeared relatively independent of the detection angle, there was a sinusoidal variation of intensity with the detection angle for the polarized PL emission for the 2D sample purified with EtOH (bottom traces). Such an observation is quite similar to the data reported for CdSe nanorods,[58] and $CH_3NH_3PbBr_3$ nanodots and nanoplatelets.[61] Thus, Figure 5 demonstrates that the as-synthesized and EtOH-purified CdSe NCs have different structural anisotropy, in agreement with our TEM results (shown by Figures 3 and 4). Additional polarized emission data for carboxylate ligand passivated CdSe NCs (purified with CH_3CN and EtOH) are shown in Figure S5-1. When the purified sample was stored for a much longer period (such as 5 days), the variation with the detection angle dependence of the polarized emission became more marked. The result shown in Figure S5-1 supports our hypothesis that storage time (before the preparation of TEM grids) promotes geometric anisotropy. In our previous TEM study,[30,32] where these effects were not considered, the use of a short-chain alcohol played a critical role in the formation and visualization of 2D wells in addition to 0D NCs; furthermore, the unintentional storage of a dispersion was probably also a contributing factor to the formation of 2D wells. A self-assembly may take place in dispersion and during drying (along with the concentration increase caused by evaporation such as TEM grid preparation);[62,63] for the present study, we focus only on the former situation.

It is curious that the 0D NCs with 3D quantum confinement and assembled 2D wells with 1D quantum confinement exhibit similar static optical features, notably in their absorption and emission spectra. Meanwhile, their polarized emission features different detection angle dependence. It is noteworthy that other 0D NCs and their assembled 2D NCs were also reported to exhibit similar bandgap regarding absorption and emission peak positions monitored, such as for colloidal halide perovskites,[61] CdTe,[25] and PbS.[26] Interestingly, there appears to be a large experimental window in which we can synthesize

NCs exhibiting sharp absorption doublets.[29−39,54,64] To understand the origin of the sharp absorption doublet, further sophistication in theoretical modeling is probably required. The uncertainty (for example in dealing with 0D and 2D NCs with strong quantum confinement along with some degree of anisotropic nature) is most likely the cause of the significant differences between theory and experiment, and among theories.

■ DISCUSSION

We would like to address related theoretical studies published. In the case of the carboxylic-ligand passivated CdSe NCs that exhibit a sharp absorption doublet at ∼460 and ∼432 nm, the thickness of the nanoplatelets was previously calculated to be six monolayers (MLs) with the parabolic model,[31] and five monolayers with the multiband effective-mass approximation model.[35] In both the calculations, a monolayer thickness (0.304 nm) was defined to be half the lattice constant of zinc-blende CdSe.[31] However, these two calculated thickness values are not consistent with the thickness derived from a TEM study which showed three monolayers.[38] Nevertheless, the difference can be attributable to model inaccuracies.

The two theoretical calculations were repeated and compared with the published experimental data.[31,35] In this regard, Figure 6a shows the calculations for the bandgap absorption (eV, y axis) versus the thickness of the 2D nanoplatelets (nm, x axis). The dashed and dotted gray curves represent the calculation obtained by the parabolic and multiband effective-mass approximation models, respectively. The variation from the two models is apparent, particularly when the thickness is less than 3 nm. Furthermore, the thicknesses reported by refs 31 and 35 were indicated and represented by the solid triangular and square symbols, respectively, for the nanoplatelets exhibiting the first exctionic absorption peaks at 392 nm (3.17 eV), 463 nm (2.68 eV), 512 nm (2.42 eV), and 550 nm (2.25 eV). The thicknesses obtained and derived by experimental TEM data in ref 38 were represented by red solid and open star symbols, respectively. The inset contains a scale expansion for the thicknesses below 3 nm, with the corresponding absorption peak position in

wavelength (nm) indicated and the parallel four lines for eye guidance. The integer numbers 2−8 represent those monolayer numbers reported by refs 31 and 35, together with those based on TEM reported by ref 38. Although the triangles are almost on the dashed line, and the squares on the dotted line, the reported thickness values (by the triangles and squares) are notably different from the data represented by the solid and open star symbols.

These differences could be understood, if we consider the nature of the corresponding original two models.[65,66] First, spherical particles were addressed originally in the parabolic model and in the multiband effective-mass approximation model.[65,66] Apparently, deficiencies can be generated when describing 2D systems (owing to the difference between the wave functions in 0D and 2D NCs). In the calculation of the thickness of 2D QWs, the radius of a sphere in the original parabolic model was simply used for the thickness of the 2D QWs.[31,63] To be consistent with the formation pathway proposed of the wells,[62] the thickness of the wells should be similar to the diameter of their seeds instead of their radius. For the multiband effective-mass approximation model, the Kane parameter E_p describing the coupling between the conduction and valence bands, was allowed to be somewhat adjustable.[35,66] This was to account for the fact that the E_p value for zinc-blende CdSe was experimentally unavailable.[35]

Second, the two models were proposed with wave vectors to determine band structures for relatively large spherical semiconductors.[65,66] The use of wave vectors has limitations for 0D NCs with 3D quantum confinement as well as for 2D NCs with 1D quantum confinement. In Figure 6b, the two calculations on bandgap absorption (eV, y axis) versus dot diameter (nm, x axis) with the parabolic and the multiband effective-mass approximation models are contained in the dashed and dotted gray curves, respectively. Also, the two empirical equations proposed previously are indicated by the green and dark-red curves.[52,53] They were developed to describe the relationship between the absorption peak position and the size of 0D QDs, according to optical absorption and TEM data. The red solid ball represents our 0D NCs imaged by TEM in Figures 3 and 4 with the absorption doublet shown in Figure 3a. The inset is an enlargement for sizes below 3 nm. The red solid ball seems to sit on the dark-red and green traces, being away from the dashed and dotted traces. Thus, these two empirical equations match our experimental data of the 0D NCs much better than either of the two band models.[65,66] The extension of the two band models to calculate the optical transition energies for our CdSe small-size 0D QDs appears to be a stretch. A more in-depth review of the two models[31,35] can be found in the Supporting Information.

CONCLUSIONS

In this study, we have shown that the as-prepared amine-ligand passivated CdSe NCs (without purification), dispersed in either toluene or hexane, exhibited a sharp absorption doublet peaked at 453 and 426 nm, and were mainly 0D NCs. However, when placed in a dispersion containing HDA, both 0D and 2D NCs were observed under TEM and subsequent dispersion sonication facilitated the presence of 2D NCs. The underlying causes for the combined morphological effect of HDA and sonication are under further exploration; in fact, sonication-induced self-assembly was reported previously.[67] Also, we have shown that the as-prepared carboxylate-ligand passivated CdSe NCs (without purification), dispersed in either toluene or

hexane, exhibited a sharp absorption doublet peaked at ∼432 and ∼460 nm, and again were mainly 0D NCs. We demonstrated when the aprotic agent acetonitrile CH_3CN was used during purification, the 0D NCs remained intact. On the other hand, when the protic agent EtOH was used, the formation of 2D wells was observed. We found out that dispersion storage time also promoted the formation of the 2D wells. Importantly, the present study suggests that the self-assembly of 0D NCs into 2D wells can be induced by an appropriate post-treatment. This effect can be exploited to engineer a targeted morphology for a particular application. Further study is evidently required regarding the assembly pathway, in which the thickness of the 2D wells that resulted seems to be smaller than the diameter of the 0D NCs. Accordingly, efforts can be directed to control the self-assembly of the Cd-based 0D NCs. On a side note, there are indications that prewires and nanorods exhibit a similar absorption doublet.[68−70] These two wire-related and rod-related observations are perhaps not totally surprising, as a possible pathway for the self-assembly of 0D NCs to 2D NCs may go through such as the 1D prewires (by the interconnection of 0D NCs). We are actively studying such a possible pathway. Although not discussed in detail here, 0D NCs can be somewhat geometrically anisotropic, a property that could provide the basis for self-assembly of 0D NCs into 2D NCs. The present study indicates the necessity for a better understanding of why a sharp absorption doublet occurs for CdSe 0D and their self-assembled 2D NCs. In general, the present study calls for experimental (including single particle absorption spectroscopy[71]) and theoretical efforts to more accurately understand how structure and optical properties are related in the 0D NCs and their assembled 2D NCs that characteristically exhibit similar sharp absorption doublets.

■ ASSOCIATED CONTENT

Ⓢ Supporting Information

The Supporting Information is available free of charge on the ACS Publications website at DOI: 10.1021/acs.chemmater.7b04645.

Methods, absorption spectra, TEM images, and polarized emission spectra (PDF)

■ AUTHOR INFORMATION

Corresponding Authors
*S. Han. E-mail: shuohan@scu.edu.cn.
*K. Yu. E-mail: kuiyu@scu.edu.cn.

ORCID Ⓘ
Hongsong Fan: 0000-0003-3812-9208
Renchao Che: 0000-0003-4192-7278
Shuo Han: 0000-0003-0880-1833
Kui Yu: 0000-0003-0349-2680

Notes
The authors declare no competing financial interest.

■ REFERENCES

(1) Grivas, C.; Li, C.; Andreakou, P.; Wang, P.; Ding, M.; Brambilla, G.; Manna, L.; Lagoudakis, P. Single-Mode Tunable Laser Emission in the Single-Exciton Regime from Colloidal Nanocrystals. *Nat. Commun.* 2013, 4, 2376−2384.

(2) Tan, C. K.; Tansu, N. Electrons and Holes Get Closer. *Nat. Nanotechnol.* 2015, 10, 107−109.

(3) Li, M.; Zhi, M.; Zhu, H.; Wu, W. Y.; Xu, Q. H.; Jhon, M. H.; Chan, Y. Ultralow-Threshold Multiphoton-Pumped Lasing from Colloidal Nanoplatelets in Solution. *Nat. Commun.* 2015, 6, 8513−8520.

(4) Reineke, S. Complementary LED Technologies. *Nat. Mater.* 2015, 14, 459−462.

(5) Yang, Z.; Voznyy, O.; Liu, M.; Yuan, M.; Ip, A. H.; Ahmed, O. S.; Levina, L.; Kinge, S.; Hoogland, S.; Sargent, E. H. All-Quantum-Dot Infrared Light-Emitting Diodes. *ACS Nano* 2015, 9, 12327−12333.

(6) Cho, I.; Jung, H.; Jeong, B. G.; Chang, J. H.; Kim, Y.; Char, K.; Lee, D. C.; Lee, C.; Cho, J.; Bae, W. K. Multifunctional Dendrimer Ligands for High-Efficiency, Solution-Processed Quantum Dot Light-Emitting Diodes. *ACS Nano* 2017, 11, 684−692.

(7) Kim, D.; Fu, Y.; Kim, S.; Lee, W.; Lee, K. H.; Chung, H. K.; Lee, H. J.; Yang, H.; Chae, H. Polyethylenimine Ethoxylated-Mediated All-Solution-Processed High-Performance Flexible Inverted Quantum Dot-Light-Emitting Device. *ACS Nano* 2017, 11, 1982−1990.

(8) Lan, X.; Masala, S.; Sargent, E. H. Charge-Extraction Strategies for Colloidal Quantum Dot Photovoltaics. *Nat. Mater.* 2014, 13, 233−240.

(9) Chuang, C. H. M.; Brown, P. R.; Bulovic, V.; Bawendi, M. G. Improved Performance and Stability in Quantum Dot Solar Cells through Band Alignment Engineering. *Nat. Mater.* 2014, 13, 796−801.

(10) Pan, Z.; Mora-Seró, I.; Shen, Q.; Zhang, H.; Li, Y.; Zhao, K.; Wang, J.; Zhong, X.; Bisquert, J. High-Efficiency "Green" Quantum Dot Solar Cells. *J. Am. Chem. Soc.* 2014, 136, 9203−9210.

(11) Fountaine, T. J.; Wincovitch, S. M.; Geho, D. H.; Garfield, S. H.; Pittaluga, S. Multispectral Imaging of Clinically Relevant Cellular Targets in Tonsil and Lymphoid Tissue Using Semiconductor Quantum Dots. *Mod. Pathol.* 2006, 19, 1181−1191.

(12) Yu, J. H.; Kwon, S. H.; Petrášek, Z.; Park, O. K.; Jun, S. W.; Shin, K.; Choi, M.; Park, Y. I.; Park, K.; Na, H. B.; Lee, N.; Lee, D. W.; Kim, J. H.; Schwille, P.; Hyeon, T. High-Resolution Three-Photon Biomedical Imaging Using Doped ZnS Nanocrystals. *Nat. Mater.* 2013, 12, 359−366.

(13) Ming, K.; Kim, J.; Biondi, M. J.; Syed, A.; Chen, K.; Lam, A.; Ostrowski, M.; Rebbapragada, A.; Feld, J. J.; Chan, W. C. W. Integrated Quantum Dot Barcode Smartphone Optical Device for Wireless Multiplexed Diagnosis of Infected Patients. *ACS Nano* 2015, 9, 3060−3074.

(14) Murray, C. B.; Norris, D. J.; Bawendi, M. G. Synthesis and Characterization of Nearly Monodisperse CdE (E = S, Se, Te) Semiconductor Nanocrystallites. *J. Am. Chem. Soc.* 1993, 115, 8706−8715.

(15) Peng, Z. A.; Peng, X. Formation of High-Quality CdTe, CdSe, and CdS Nanocrystals Using CdO as Precursor. *J. Am. Chem. Soc.* 2001, 123, 183−184.

(16) Yu, K.; Hrdina, A.; Ouyang, J.; Kingston, D.; Wu, X.; Leek, D. M.; Liu, X.; Li, C. Ultraviolet $ZnSe_{1-x}S_x$ Gradient-Alloyed Nanocrystals

via a Noninjection Approach. *ACS Appl. Mater. Interfaces* 2012, 4, 4302−4311.

(17) Yu, K.; Ng, P.; Ouyang, J.; Zaman, M. B.; Abulrob, A.; Baral, T. N.; Fatehi, D.; Jakubek, Z. J.; Kingston, D.; Wu, X.; Liu, X.; Hebert, C.; Leek, D. M.; Whitfield, D. M. Low-Temperature Approach to Highly Emissive Copper Indium Sulfide Colloidal Nanocrystals and Their Bioimaging Applications. *ACS Appl. Mater. Interfaces* 2013, 5, 2870−2880.

(18) Hendricks, M. P.; Campos, M. P.; Cleveland, G. T.; Plante, I. J. L.; Owen, J. S. A Tunable Library of Substituted Thiourea Precursors to Metal Sulfide Nanocrystals. *Science* 2015, 348, 1226−1230.

(19) Cooper, J. K.; Gul, S.; Lindley, S. A.; Yano, J.; Zhang, J. Z. Tunable Photoluminescent Core/Shell Cu^+-Doped ZnSe/ZnS Quantum Dots Codoped with Al^{3+}, Ga^{3+}, or In^{3+}. *ACS Appl. Mater. Interfaces* 2015, 7, 10055−10066.

(20) Zhang, J.; Yang, Q.; Cao, H.; Ratcliffe, C. I.; Kingston, D.; Chen, Q. Y.; Ouyang, J.; Wu, X.; Leek, D. M.; Riehle, F. S.; Yu, K. Bright Gradient-Alloyed $CdSe_xS_{1-x}$ Quantum Dots Exhibiting Cyan-Blue Emission. *Chem. Mater.* 2016, 28, 618−625.

(21) Wang, F.; Tang, R.; Buhro, W. E. The Trouble with TOPO; Identification of Adventitious Impurities Beneficial to the Growth of Cadmium Selenide Quantum Dots, Rods, and Wires. *Nano Lett.* 2008, 8, 3521−3524.

(22) Zanella, M.; Gomes, R.; Povia, M.; Giannini, C.; Zhang, Y.; Riskin, A.; Van Bael, M.; Hens, Z.; Manna, L. Self-Assembled Multilayers of Vertically Aligned Semiconductor Nanorods on Device-Scale Areas. *Adv. Mater.* 2011, 23, 2205−2209.

(23) Wang, F.; Buhro, W. E. Crystal-Phase Control by Solution−Solid−Solid Growth of II−VI Quantum Wires. *Nano Lett.* 2016, 16, 889−894.

(24) Wang, F.; Dong, A.; Buhro, W. E. Solution−Liquid−Solid Synthesis, Properties, and Applications of One-Dimensional Colloidal Semiconductor Nanorods and Nanowires. *Chem. Rev.* 2016, 116, 10888−10933.

(25) Tang, Z.; Zhang, Z.; Wang, Y.; Glotzer, S. C.; Kotov, N. A. Self-Assembly of CdTe Nanocrystals into Free-Floating Sheets. *Science* 2006, 314, 274−278.

(26) Schliehe, C.; Juarez, B. H.; Pelletier, M.; Jander, S.; Greshnykh, D.; Nagel, M.; Meyer, A.; Foerster, S.; Kornowski, A.; Klinke, C.; Weller, H. Ultrathin PbS Sheets by Two-Dimensional Oriented Attachment. *Science* 2010, 329, 550−553.

(27) Du, Y.; Yin, Z.; Zhu, J.; Huang, X.; Wu, X. J.; Zeng, Z.; Yan, Q.; Zhang, H. A General Method for the Large-Scale Synthesis of Uniform Ultrathin Metal Sulphide Nanocrystals. *Nat. Commun.* 2012, 3, 1177−1183.

(28) Mu, L.; Wang, F.; Sadtler, B.; Loomis, R. A.; Buhro, W. E. Influence of the Nanoscale Kirkendall Effect on the Morphology of Copper Indium Disulfide Nanoplatelets Synthesized by Ion Exchange. *ACS Nano* 2015, 9, 7419−7428.

(29) Joo, J.; Son, J. S.; Kwon, S. G.; Yu, J. H.; Hyeon, T. Low-Temperature Solution-Phase Synthesis of Quantum Well Structured CdSe Nanoribbons. *J. Am. Chem. Soc.* 2006, 128, 5632−5633.

(30) Ouyang, J.; Zaman, M. B.; Yan, F. J.; Johnston, D.; Li, G.; Wu, X.; Leek, D.; Ratcliffe, C. I.; Ripmeester, J. A.; Yu, K. Multiple Families of Magic-Sized CdSe Nanocrystals with Strong Bandgap Photoluminescence via Noninjection One-Pot Syntheses. *J. Phys. Chem. C* 2008, 112, 13805−13811.

(31) Ithurria, S.; Dubertret, B. Quasi 2D Colloidal CdSe Platelets with Thicknesses Controlled at the Atomic Level. *J. Am. Chem. Soc.* 2008, 130, 16504−16505.

(32) Yu, K.; Ouyang, J.; Zaman, M. B.; Johnston, D.; Yan, F. J.; Li, G.; Ratcliffe, C. I.; Leek, D. M.; Wu, X.; Stupak, J.; Jakubek, Z.; Whitfield, D. Single-Sized CdSe Nanocrystals with Bandgap Photoemission via a Noninjection One-Pot Approach. *J. Phys. Chem. C* 2009, 113, 3390−3401.

(33) Wang, R.; Ouyang, J.; Nikolaus, S.; Brestaz, L.; Zaman, M. B.; Wu, X.; Leek, D.; Ratcliffe, C. I.; Yu, K. Single-Sized Colloidal CdTe Nanocrystals with Strong Bandgap Photoluminescence. *Chem. Commun.* 2009, 8, 962−964.

(34) Wang, R.; Calvignanello, O.; Ratcliffe, C. I.; Wu, X.; Leek, D. M.; Zaman, M. B.; Kingston, D.; Ripmeester, J. A.; Yu, K. Homogeneously-Alloyed CdTeSe Single-Sized Nanocrystals with Bandgap Photoluminescence. *J. Phys. Chem. C* **2009**, *113*, 3402−3408.

(35) Ithurria, S.; Tessier, M. D.; Mahler, B.; Lobo, R. P. S. M.; Dubertret, B.; Efros, A. L. Colloidal Nanoplatelets with Two-Dimensional Electronic Structure. *Nat. Mater.* **2011**, *10*, 936−941.

(36) Li, Z.; Peng, X. Size/Shape-Controlled Synthesis of Colloidal CdSe Quantum Disks: Ligand and Temperature Effects. *J. Am. Chem. Soc.* **2011**, *133*, 6578−6586.

(37) Yu, K. CdSe Magic-Sized Nuclei, Magic-Sized Nanoclusters and Regular Nanocrystals: Monomer Effects on Nucleation and Growth. *Adv. Mater.* **2012**, *24*, 1123−1132.

(38) Mahler, B.; Nadal, B.; Bouet, C.; Patriarche, G.; Dubertret, B. Core/Shell Colloidal Semiconductor Nanoplatelets. *J. Am. Chem. Soc.* **2012**, *134*, 18591−18598.

(39) Liu, Y. H.; Wang, F.; Wang, Y.; Gibbons, P. C.; Buhro, W. E. Lamellar Assembly of Cadmium Selenide Nanoclusters into Quantum Belts. *J. Am. Chem. Soc.* **2011**, *133*, 17005−17013.

(40) Li, M.; Ouyang, J.; Ratcliffe, C. I.; Pietri, L.; Wu, X.; Leek, D. M.; Moudrakovski, I.; Lin, Q.; Yang, B.; Yu, K. CdS Magic-Sized Nanocrystals Exhibiting Bright Band Gap Photoemission via Thermodynamically Driven Formation. *ACS Nano* **2009**, *3*, 3832−3838.

(41) Wang, R.; Ratcliffe, C. I.; Wu, X.; Voznyy, O.; Tao, Y.; Yu, K. Magic-Sized Cd_3P_2 II-V Nanoparticles Exhibiting Bandgap Photoemission. *J. Phys. Chem. C* **2009**, *113*, 17979−17982.

(42) Kudera, S.; Zanella, M.; Giannini, C.; Rizzo, A.; Li, Y.; Gigli, G.; Cingolani, R.; Ciccarella, G.; Spahl, W.; Parak, W. J.; Manna, L. Sequential Growth of Magic-Size CdSe Nanocrystals. *Adv. Mater.* **2007**, *19*, 548−552.

(43) Empedocles, S. A.; Neuhauser, R.; Shimizu, K.; Bawendi, M. G. Photoluminescence from Single Semiconductor Nanostructures. *Adv. Mater.* **1999**, *11*, 1243−1256.

(44) Cui, J.; Beyler, A. P.; Marshall, L. F.; Chen, O.; Harris, D. K.; Wanger, D. D.; Brokmann, X.; Bawendi, M. G. Direct Probe of Spectral Inhomogeneity Reveals Synthetic Tunability of Single-Nanocrystal Spectral Linewidths. *Nat. Chem.* **2013**, *5*, 602−606.

(45) Grim, J. Q.; Christodoulou, S.; Di Stasio, F.; Krahne, R.; Cingolani, R.; Manna, L.; Moreels, I. Continuous-Wave Biexciton Lasing at Room Temperature Using Solution-Processed Quantum Wells. *Nat. Nanotechnol.* **2014**, *9*, 891−895.

(46) She, C.; Fedin, I.; Dolzhnikov, D. S.; Demortière, A.; Schaller, R. D.; Pelton, M.; Talapin, D. V. Low-Threshold Stimulated Emission Using Colloidal Quantum Wells. *Nano Lett.* **2014**, *14*, 2772−2777.

(47) Guzelturk, B.; Kelestemur, Y.; Olutas, M.; Delikanli, S.; Demir, H. V. Amplified Spontaneous Emission and Lasing in Colloidal Nanoplatelets. *ACS Nano* **2014**, *8*, 6599−6605.

(48) She, C.; Fedin, I.; Dolzhnikov, D. S.; Dahlberg, P. D.; Engel, G. S.; Schaller, R. D.; Talapin, D. V. Red, Yellow, Green, and Blue Amplified Spontaneous Emission and Lasing Using Colloidal CdSe Nanoplatelets. *ACS Nano* **2015**, *9*, 9475−9485.

(49) Hassinen, A.; Moreels, I.; De Nolf, K.; Smet, P. F.; Martins, J. C.; Hens, Z. Short-Chain Alcohols Strip X-Type Ligands and Quench the Luminescence of PbSe and CdSe Quantum Dots, Acetonitrile Does Not. *J. Am. Chem. Soc.* **2012**, *134*, 20705−20712.

(50) Anderson, N. C.; Hendricks, M. P.; Choi, J. J.; Owen, J. S. Ligand Exchange and the Stoichiometry of Metal Chalcogenide Nanocrystals: Spectroscopic Observation of Facile Metal-Carboxylate Displacement and Binding. *J. Am. Chem. Soc.* **2013**, *135*, 18536−18548.

(51) Yang, Y.; Li, J.; Lin, L.; Peng, X. An Efficient and Surface-Benign Purification Scheme for Colloidal Nanocrystals Based on Quantitative Assessment. *Nano Res.* **2015**, *8*, 3353−3364.

(52) Yu, W. W.; Qu, L.; Guo, W.; Peng, X. Experimental Determination of the Extinction Coefficient of CdTe, CdSe, and CdS Nanocrystals. *Chem. Mater.* **2003**, *15*, 2854−2860.

(53) Jasieniak, J.; Smith, L.; van Embden, J.; Mulvaney, P.; Califano, M. Re-Examination of the Size-Dependent Absorption Properties of CdSe Quantum Dots. *J. Phys. Chem. C* **2009**, *113*, 19468−19474.

(54) Yu, J. H.; Liu, X.; Kweon, K. E.; Joo, J.; Park, J.; Ko, K. T.; Lee, D. W.; Shen, S.; Tivakornsasithorn, K.; Son, J. S.; Park, J. H.; Kim, Y. W.; Hwang, G. S.; Dobrowolska, M.; Furdyna, J. K.; Hyeon, T. Giant Zeeman Splitting in Nucleation-Controlled Doped CdSe: Mn^{2+} Quantum Nanoribbons. *Nat. Mater.* **2010**, *9*, 47−53.

(55) Owen, J. S.; Chan, E. M.; Liu, H.; Alivisatos, A. P. Precursor Conversion Kinetics and the Nucleation of Cadmium Selenide Nanocrystals. *J. Am. Chem. Soc.* **2010**, *132*, 18206−18213.

(56) Liu, M.; Wang, K.; Wang, L.; Han, S.; Fan, H.; Rowell, N.; Ripmeester, J. A.; Renoud, R.; Bian, F.; Zeng, J.; Yu, K. Probing Intermediates of the Induction Period Prior to Nucleation and Growth of Semiconductor Quantum Dots. *Nat. Commun.* **2017**, *8*, 15467.

(57) Zhu, T.; Zhang, B.; Zhang, J.; Lu, J.; Fan, H.; Rowell, N.; Ripmeester, J. A.; Han, S.; Yu, K. Two-Step Nucleation of CdS Magic-Size Nanocluster MSC−311. *Chem. Mater.* **2017**, *29*, 5727−5735.

(58) Hu, J.; Li, L. S.; Yang, W.; Manna, L.; Wang, L. W.; Alivisatos, A. P. Linearly Polarized Emission from Colloidal Semiconductor Quantum Rods. *Science* **2001**, *292*, 2060−2063.

(59) Tiwari, V.; Solanki, V. Fluorescence Studies for Biomolecular Structure and Dynamics. In *Reviews in Fluorescence 2016*; Geddes, C. D., Ed.; Springer, 2017; pp 319−357.

(60) Basu, P.; Kumar, G. S. A Comparative Study on the Interaction of the Putative Anticancer Alkaloids, Sanguinarine and Chelerythrine, with Single- and Double-Stranded, and Heat-Denatured DNAs. *J. Biomol. Struct. Dyn.* **2015**, *33*, 2594−2605.

(61) Liu, L.; Huang, S.; Pan, L.; Shi, L. J.; Zou, B.; Deng, L.; Zhong, H. Colloidal Synthesis of $CH_3NH_3PbBr_3$ Nanoplatelets with Polarized Emission through Self-Organization. *Angew. Chem., Int. Ed.* **2017**, *56*, 1780−1783.

(62) Zhang, L.; Yu, K.; Eisenberg, A. Ion-Induced Morphological Changes in "Crew-Cut" Aggregates of Amphiphilic Block Copolymers. *Science* **1996**, *272*, 1777−1779.

(63) Yu, K.; Hurd, A. J.; Eisenberg, A.; Brinker, C. J. Syntheses of Silica/Polystyrene-*Block*-Poly(ethylene oxide) Films with Regular and Reverse Mesostructures of Large Characteristic Length Scales by Solvent Evaporation-Induced Self-Assembly. *Langmuir* **2001**, *17*, 7961−7965.

(64) Ithurria, S.; Bousquet, G.; Dubertret, B. Continuous Transition from 3D to 1D Confinement Observed During the Formation of CdSe Nanoplatelets. *J. Am. Chem. Soc.* **2011**, *133*, 3070−3077.

(65) Brus, L. Electronic Wave Functions in Semiconductor Clusters: Experiment and Theory. *J. Phys. Chem.* **1986**, *90*, 2555−2560.

(66) Efros, A. L.; Rosen, M. Quantum Size Level Structure of Narrow-Gap Semiconductor Nanocrystals: Effect of Band Coupling. *Phys. Rev. B: Condens. Matter Mater. Phys.* **1998**, *58*, 7120−7135.

(67) Deng, C.; Fang, R.; Guan, Y.; Jiang, J.; Lin, C.; Wang, L. Sonication-Induced Self-Assembly of Flexible Tris(ureidobenzyl)-amine: from Dimeric Aggregates to Supramolecular Gels. *Chem. Commun.* **2012**, *48*, 7973−7975.

(68) Zhang, L. J.; Shen, X.-C.; Liang, H.; Yao, J.-T. Multiple Families of Magic-Sized ZnSe Quantum Dots via Noninjection One-Pot and Hot-Injection Synthesis. *J. Phys. Chem. C* **2010**, *114*, 21921−21927.

(69) Pradhan, N.; Xu, H.; Peng, X. Colloidal CdSe Quantum Wires by Oriented Attachment. *Nano Lett.* **2006**, *6*, 720−724.

(70) The most critical *JACS* reviewer brought our attention to cite ref 69. After an extremely careful study, we found out that the parts of Figure 2 top-right and bottom panels provide absorption spectra that have the absorption doublet peaking at ∼430 and ∼ 461 nm. And prewires (the pearl-necklace-shaped nanowires) and magic-size clusters were assigned to be the origin of the absorption doublet. It was claimed that "each prewire aggregate should consist of many magic-sized clusters".

(71) McDonald, M. P.; Chatterjee, R.; Si, J.; Jankó, B.; Kuno, M. Dimensional Crossover in Semiconductor Nanostructures. *Nat. Commun.* **2016**, *7*, 12726.